

Steric Manipulation of the Reductive Reactivity of Ytterbocenes toward 2-(((2,6-Diisopropylphenyl)imino)methyl)pyridine: Insertion of the N=C Bond into the Yb–Indenyl Bond or Oxidative Cleavage of the η^5 Yb–Cp (Cp = C₁₃H₉, Cp*) Bond

Alexander A. Trifonov,^{*,†} Elena A. Fedorova,[†] Ivan A. Borovkov,[†] Georgy K. Fukin,[†] Evguenii V. Baranov,[†] Joulia Larionova,[‡] and Nikolai O. Druzhkov[†]

G.A. Razuvaev Institute of Organometallic Chemistry of Russian Academy of Sciences, Tropinina 49, GSP-445, 603950 Nizhny Novgorod, Russia, and Laboratoire de Chimie Moléculaire et Organisation du Solide, Batiment 17, Case Courrier 007, Place Eugene Bataillon, F-34095 Montpellier Cedex 5, France

Received January 24, 2007

Summary: Unprecedented N=C bond insertion into the η^5 Yb–C₉H₇ bond occurs in the reaction of 2-(((2,6-diisopropylphenyl)imino)methyl)pyridine with (C₉H₇)₂Yb(THF)₂ and affords the Yb(III) derivative [Yb(η^5 -C₉H₇){N(2,6-*i*-Pr₂C₆H₃)CH(C₉H₇)-(C₅H₄N)}₂]{2,6-*i*-Pr₂C₆H₃NCH(C₅H₄N)^{•-}}. For the complexes Cp₂Yb(THF)₂ (Cp = C₁₃H₉, Cp*) coordinated by bulkier η^5 ligands the same reaction results in an oxidative cleavage of the η^5 Yb–Cp (Cp = C₁₃H₉, Cp*) bond and formation of [Yb{(2,6-*i*-Pr₂C₆H₃NCH(C₅H₄N)^{•-})₃] and [Yb(C₅Me₅){(2,6-*i*-Pr₂C₆H₃NCH(C₅H₄N)^{•-})₂}, respectively.

Ytterbocenes have demonstrated rich and intriguing reductive reactivity toward α,α' -diimines.^{1–3} These reactions are found to be strongly influenced by steric crowding in the coordination sphere of the ytterbium atom. The reaction pathway can be dramatically changed by modification of the steric demand of both carbocyclic ligands η^5 coordinated to the ytterbium atom and substituents at nitrogens of the diimine molecule. *t*-BuN=CHCH=N-*t*-Bu (DAB) oxidizes ytterbocenes Cp₂Yb(THF)₂ (Cp = C₅H₅,^{1a} C₅Me₅,^{1b} C₉H₇,^{1c} CH₂-1-C₉H₆^{1c}), affording the metallocene-type complexes Cp₂Yb(DAB^{•-}) coordinated by the radical anionic diazabutadiene ligand. The bulkier diazabutadiene *i*-Pr₂C₆H₃N=CHCH=NC₆H₃-*i*-Pr₂-2,6 (DAD) reacts with the bis(indenyl) derivative (C₉H₇)₂Yb(THF)₂, affording the oxidation product (C₉H₇)₂Yb(DAD^{•-}),^{2a} while the reaction with the analogue (C₁₃H₉)₂Yb(THF)₂, containing more sterically demanding fluorenyl ligands, resulted in C–C coupling and formation of the unusual Yb^{II} complex [Yb{ η^5 -C₁₃H₈C(=N–C₆H₃-*i*-Pr₂-2,6)CH₂NHC₆H₃-*i*-Pr₂-2,6}](THF).^{2b} Moreover, ytterbocenes can act as both one- and two-electron reductants in their reactions with DAD.^{2c} The complex (C₅MeH₄)₂Yb(THF)₂

reduces DAD to a radical anion, and the Yb^{III} derivative (C₅MeH₄)₂Yb(DAD^{•-}) forms. In contrast, the compounds Cp^{*2}-Yb(THF)₂ (Cp* = C₅Me₅, C₅Me₄H), containing bulkier cyclopentadienyl ligands, under similar conditions act as two-electron reductants. The reactions lead to abstraction of one Cp* ring and afforded the Yb^{III} complexes [YbCp*(DAD)(THF)], coordinated by the dianion of DAD. Obviously the complexes Cp^{*2}-Yb(THF)₂ demonstrate sterically induced reductive reactivity,⁴ and double reduction of DAD becomes possible due to oxidation of the Yb^{II} to Yb^{III} and oxidation of one Cp* anion. In order to gain better insight into the factors determining the variety of pathways of reactions of ytterbocenes with diimines, we explored interactions of the complexes Cp''₂Yb(THF)₂ (Cp'' = C₉H₇ (**1**), C₁₃H₉ (**2**), C₅Me₅ (**3**)) η^5 -coordinated by monoanionic ligands possessing different size and coordination capacities with 2-(((2,6-diisopropylphenyl)imino)methyl)pyridine (**4**).

The reaction of the bis(indenyl) derivative **1** with 2 equiv of **4** (THF, 20 °C) led to formation of the Yb(III) complex [Yb(η^5 -C₉H₇){N(2,6-*i*-Pr₂C₆H₃)CH(C₉H₇)(C₅H₅N)}₂]{2,6-*i*-Pr₂C₆H₃NCH(C₅H₅N)^{•-}} (**5**), which was isolated in 61% yield (Scheme 1).

The paramagnetism of complex **5** ($\mu_{\text{eff}} = 4.3 \mu\text{B}$, 293 K) indicates the trivalent oxidation state of the ytterbium atom.⁵ The X-ray diffraction study (Figure 1) revealed that the coordination sphere of the Yb atom in complex **5** is made up of a η^5 -coordinated C₉H₇ anion, two N atoms of the amido-pyridinato ligand, and two N atoms of the iminopyridine radical anion. The chelating amido-pyridinato ligand arises from insertion of the N=C bond of **4** into the Yb–C₉H₇ bond. This insertion results in Yb–C₉H₇ bond cleavage and formation of Yb–N and C–C bonds. To the best of our knowledge, this is the sole example of such an insertion. The amido-pyridinato ligand is bound to the Yb atom by one covalent (Yb(1)–N(4) = 2.195(2) Å) and one coordination (Yb(1)–N(3) = 2.397(2) Å) Yb–N bond.^{3a,6} The insertion leads to the change of hybridization of “ex”-imino C and N atoms.

The bond angles about the carbon atom C24 (N4–C24–C37 = 112.7(3)°, N4–C24–C23 = 111.7(2)°, N4–C24–H24 = 111.8(3)°) proves that, unlike the related carbon in the parent **4**, it adopts sp³ hybridization. The noticeable difference in bond distances between the Yb ion and the C atoms of the five-membered ring indicates a partial distortion of the indenyl ligand coordination toward an η^3 type. The shortening of the average Yb–C(C₅-indenyl) bond lengths in **5** (2.670(3) Å) compared

* To whom correspondence should be addressed. Fax: (+)(+7)-8312621497. E-mail: trif@iomc.ras.ru.

[†] G.A. Razuvaev Institute of Organometallic Chemistry of Russian Academy of Sciences.

[‡] Laboratoire de Chimie Moléculaire et Organisation du Solide.

(1) (a) Trifonov, A. A.; Kirillov, E. N.; Bochkarev, M. N.; Schumann, H.; Muehle, S. *Russ. Chem. Bull.* **1999**, *48*, 382–384. (b) Trifonov, A. A.; Kurskii, Yu. A.; Bochkarev, M. N.; Muehle, S.; Dechert, S.; Schumann, H. *Russ. Chem. Bull.* **2003**, *52*, 601–606. (c) Trifonov, A. A.; Fedorova, E. A.; Ikorskii, V. N.; Dechert, S.; Schumann, H.; Bochkarev, M. N. *Eur. J. Inorg. Chem.* **2005**, 2812–2818.

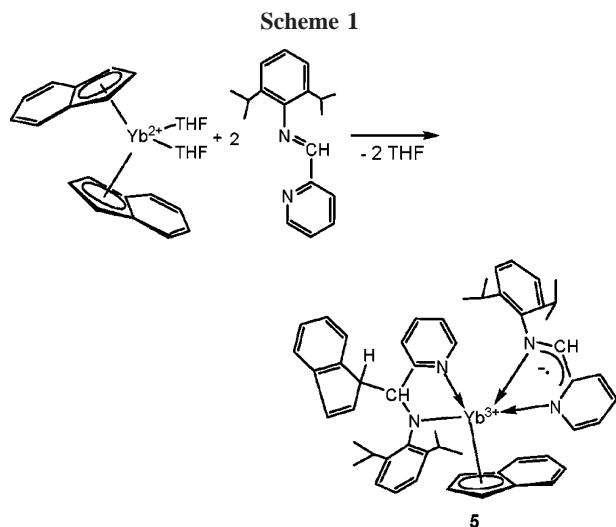
(2) (a) Trifonov, A. A.; Fedorova, E. A.; Fukin, G. K.; Ikorskii, V. N.; Kurskii, Yu. A.; Dechert, S.; Schumann, H.; Bochkarev, M. N. *Russ. Chem. Bull.* **2004**, *53*, 2736–2743. (b) Trifonov, A. A.; Fedorova, E. A.; Fukin, G. K.; Druzhkov, N. O.; Bochkarev, M. N. *Angew. Chem., Int. Ed.* **2004**, *43*, 5045–5048. (c) Trifonov, A. A.; Borovkov, I. A.; Fedorova, E. A.; Fukin, G. K.; Larionova, J.; Druzhkov, N. O.; Cherkasov, V. K. *Chem. Eur. J.*, in press.

(3) (a) Schulz, M.; Boncella, J.; Berg, D. J.; Tilley, D. T.; Andersen, R. A. *Organometallics* **2002**, *21*, 460–472. (b) Walter, M. D.; Berg, D. J.; Andersen, R. A. *Organometallics* **2006**, *25*, 3228–3237. (c) Walter, M. D.; Schulz, M.; Andersen, R. A. *New J. Chem.* **2006**, *30*, 238–246.

(4) (a) Evans, W. J.; Davis, B. L. *Chem. Rev.* **2002**, *102*, 2119–2136.

(b) Evans, W. J. *J. Organomet. Chem.* **2002**, *647*, 2–11.

(5) Evans, W. J.; Hozbor, M. A. *J. Organomet. Chem.* **1987**, *326*, 299–306.



to those in the starting ytterbocene **1** (2.73 Å)⁷ reflects the oxidation of the ytterbium atom to the Yb(III) state.⁸ The geometric parameters within the planar (deviation is 0.0001 Å) NCCN fragment of the iminopyridine ligand in **5** are noticeably different from those in d transition metal complexes with neutral **4**.⁹ Elongation of the N2–C6 bond (1.334(4) Å) and shortening of the C5–C6 bond (1.410(4) Å) compared to the appropriate distances in the complexes [FeCl₂{2,6-*i*-Pr₂C₆H₃NCH(C₅H₅N)}] (1.272(4) and 1.467(5) Å, respectively),^{9a} [PdCl₂{2,6-*i*-Pr₂C₆H₃NCH(C₅H₅N)}] (1.279(4) and 1.457(5) Å, respectively)^{9b} give evidence for the reduced radical anion character of the iminopyridine ligand in **5**. The ytterbium–nitrogen bond lengths observed in complex **5** (Yb1–N1 = 2.326(3) Å, Yb1–N2 = 2.353(3) Å) are close to the values of Yb–N coordination bond distances reported for related Yb(III) compounds.⁶ Formation of the amido–pyridinato ligand in complex **5** obviously implies rearrangement of the coordination fashion of one of the indenyl ligands in **1** from η⁵ to η¹ and subsequent insertion of the N=C bond of the iminopyridine molecule coordinated to the ytterbium atom into the Yb–C₉H₇ bond.

N=C bond insertion into a η⁵ Yb–C bond is very uncommon. In order to gain better insight into this process, we focused on reactions of (C₉H₇)₂Yb(THF)₂ with imino derivatives having similar geometries and steric demands but different substituents at the carbon atoms. Curiously, complex **1** does not react with the related imine 2,6-*i*-Pr₂C₆H₃N=CHC₆H₅ and iminothiophene 2,6-*i*-Pr₂C₆H₃N=CHC₄H₄S (1:2 molar ratio), even with prolonged heating in THF and toluene (60 °C). Obviously, both chelating effects and electron-accepting properties of the imino compound play a crucial role in the insertion process.

The reaction of the complex (C₁₃H₉)₂Yb(THF)₂ (**2**), containing more sterically demanding fluorenyl ligands, with **4** under similar conditions occurs in an absolutely different way and results in cleavage of η⁵ Yb–C₁₃H₉ bonds, oxidation of the Yb

atom to the trivalent state, and formation of the tris(iminopyridine) compound [Yb{(2,6-*i*-Pr₂C₆H₃NCH(C₅H₅N)^{•-})₃] (**6**) (Scheme 2). Fluorene was found in the reaction mixture (80%).

The value of the magnetic moment of complex **6** (3.74 μB, 293 K) gives evidence for the trivalent oxidation state of the ytterbium atom. The X-ray crystal structure determination has shown that the Yb atom in **6** is coordinated by three chelating iminopyridine ligands bound to the ytterbium atom via two nitrogen atoms (Figure 2). The Yb–N bond lengths in **6** are somewhat different (2.372(3) and 2.356(2) Å), and their values are comparable to those reported for coordination Yb–N bonds^{3a,5c} and appropriate distances in Yb(III) complexes with radical anionic diazadiene ligands.^{1b,2a} The bonding situation within the planar (the mean deviation is 0.0151 Å) diimino fragment N1–C13–C14–N2 in **6** is consistent with the radical anionic form of the iminopyridine ligand: the C–C bond (1.382(5) Å) is shorter, while the N=C bonds are longer than the appropriate bonds in the d transition-metal complexes with neutral iminopyridine ligands.⁹ The successive augmentation of the steric demand of the π-anionic ligand coordinated to the ytterbium atom and passage to the permethylated derivative (C₅Me₅)₂Yb(THF)₂ (**3**) changes dramatically the pathway of the reaction with iminopyridine. The reaction of **3** with a 2-fold molar excess of **4** under similar conditions occurs with abstraction of one Cp* ring and oxidation of the ytterbium atom and affords a novel half-sandwich complex of trivalent ytterbium, [Yb(C₅Me₅){(2,6-*i*-Pr₂C₆H₃NCH(C₅H₅N)^{•-})₂] (**7**) (Scheme 3). The value of the magnetic moment of complex **7** (3.71 μB, 293 K) is consistent with a trivalent oxidation state of the ytterbium atom.⁵ The X-ray diffraction study (Figure 3) revealed that in complex **7** the ytterbium atom is coordinated by one C₅Me₅ ligand in a η⁵ fashion and two iminopyridine radical anions. Both of the chelating iminopyridine radical anions in **7** are bound to the ytterbium atom through two coordination Yb–N bonds (Yb1–N1A = 2.356(2) Å, Yb1–N2A = 2.345(2) Å, Yb1–N1B = 2.346(2) Å, Yb1–N2B = 2.333(2) Å). There are short Yb–C contacts (Yb1–C23A = 3.142(3) Å, Yb1–C23B = 3.130(3) Å, Yb1–C24A = 3.180(2) Å, Yb1–C24B = 3.173(3) Å). The average Yb–C (Cp*) bond length in complex **7** (2.631(3) Å) is noticeably shorter than the corresponding value in the Yb^{II} complex Cp*₂Yb(py)₂ (2.74 Å)¹⁰ and comparable to those in the related Yb(III) complexes (C₅Me₅)₂YbX(L) (2.628–2.65 Å), (X = Hal, L = THF),¹¹ giving evidence of the trivalent oxidation state of the ytterbium atom in **7**. The bond distances within the diimino fragments of both iminopyridine ligands in **7** indicate their radical anionic state. Complexes **5–7** are ESR silent in the solid state and THF solution (100–293 K).

Thus, the pathway of reactions of ytterbocenes with 2-(((2,6-diisopropylphenyl)imino)methyl)pyridine is mainly defined by both steric crowding in the coordination sphere of the metal atom and the coordination capacities of the π-aromatic ligands bound to ytterbium. The reactions can result in insertion of the N=C bond into the Yb–indenyl bond or oxidative cleavage of the η⁵ Yb–Cp (Cp = C₁₃H₉, Cp*) bond. Unfortunately, at present we cannot explain which factor predominates in driving these reactions toward insertion or cleavage processes and the formation of complexes **5–7**. Undoubtedly, the initial act of the reaction is coordination of 2-(((2,6-diisopropylphenyl)imino)methyl)pyridine to the ytterbium atom and formation of the mixed-ligand derivatives. We suggest that oxidation of the

(6) For comparison, see for the covalent Yb^{III}–N bond: (a) Sheng, E.; Wang, S.; Yang, G.; Zhou, S.; Cheng, L.; Zhang, K.; Huang, Z. *Organometallics* **2003**, *22*, 684–692. (b) Wang, Y.; Shen, Q.; Xue, F.; Tu, K. *J. Organomet. Chem.* **2000**, *598*, 359–364. For the coordination Yb^{III}–N bond, see: (c) Zhou, X.; Huang, Z.; Cai, R.; Zhang, L.-B.; Zhang, L.-X.; Huang, X. *Organometallics* **1999**, *18*, 4128–4133.

(7) Jin, J. Z.; Jin, Z. S.; Chen, W. Q.; Zhang, Y. *Chin. J. Struct. Chem. (Jiegou Huaxue)* **1993**, *12*, 241–245.

(8) Shannon, R. D. *Acta Crystallogr., Sect. A* **1976**, *32*, 751–767.

(9) (a) Gibson, V. C.; O'Reilly, R. K.; Wass, D. F.; White, A. J. P.; Williams, D. J. *Dalton Trans.* **2003**, 2824–2830. (b) Laine, T. V.; Klinga, M.; Leskelä, M. *Eur. J. Inorg. Chem.* **1999**, 959–964. (c) Laine, T. V.; Piironen, U.; Lappalainen, K.; Klinga, M.; Aitolla, E.; Leskelä, M. *J. Organomet. Chem.* **2000**, *606*, 112–124.

(10) Tilley, T. D.; Andersen, R. A.; Spencer, B.; Zalkin, A. *Inorg. Chem.* **1982**, *21*, 2647–2649.

(11) (a) Watson, P. L.; Tulip, T. H.; Williams, I. *Organometallics* **1990**, *9*, 1999–2009. (b) Tilley, T. D.; Andersen, R. A.; Zalkin, A. *Inorg. Chem.* **1983**, *22*, 856–859.

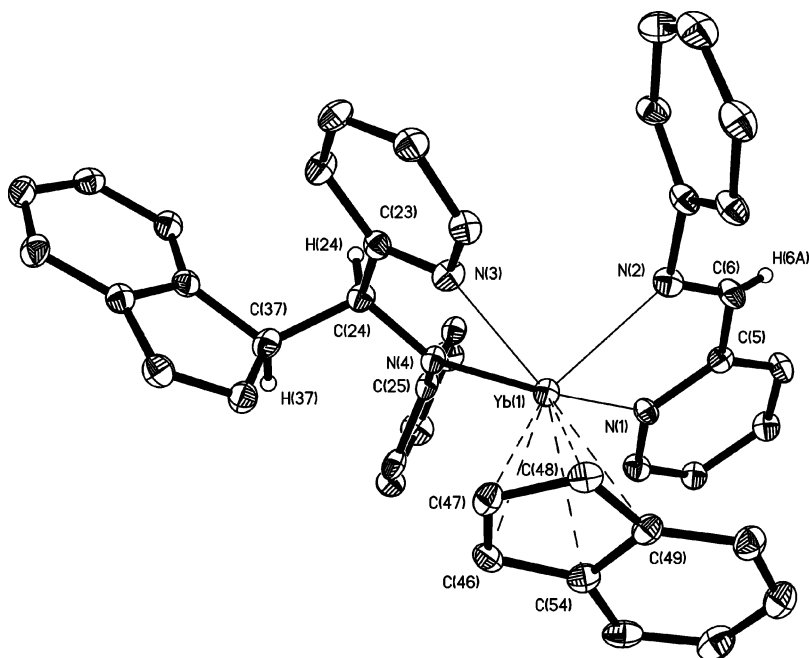
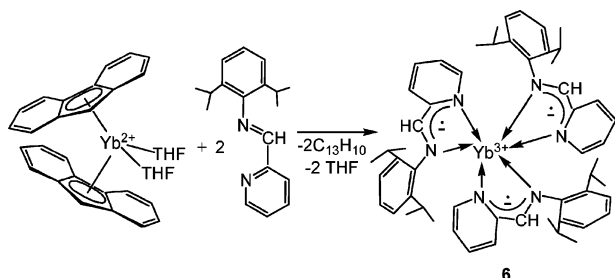


Figure 1. Molecular structure of the complex $[\text{Yb}(\eta^5\text{-C}_9\text{H}_7)\{\text{N}(2,6\text{-}i\text{-Pr}_2\text{C}_6\text{H}_3)\text{CH}(\text{C}_9\text{H}_7)(\text{C}_5\text{H}_5\text{N})\}\{\eta^4\text{-}2,6\text{-}i\text{-Pr}_2\text{C}_6\text{H}_3\text{NCH}(\text{C}_5\text{H}_5\text{N})\}]$ (**5**). Isopropyl groups of iminopyridine ligands are omitted for clarity. The terminal ellipsoids correspond to 30% probability. Selected bond lengths (Å) and angles (deg): Yb1–N4 = 2.195(2), Yb1–N3 = 2.397(2), Yb1–N1 = 2.326(2), Yb1–N2 = 2.353(3), Yb1–C47 = 2.603(3), Yb1–C46 = 2.621(3), Yb1–C48 = 2.649(3), Yb1–C54 = 2.730(3), Yb1–C49 = 2.750(3), Yb1–C5 = 3.174(3), Yb1–C6 = 3.140(3), N2–C6 = 1.334(4), C5–C6 = 1.410(4); N4–C24–C37 = 112.7(3), N4–C24–C23 = 111.7(2), N4–C24–H24 = 111.7(3), N2–C6–C5 = 121.7(3), C24–N4–C25 = 110.6(2), C25–N4–Yb1 = 126.7(2), Yb1–N4–C24 = 122.2(3), N4–C24–H24 = 111.8(2).

Scheme 2



ytterbium atom to the trivalent state occurs in this step. The tendency of the π -aromatic ligands coordinated to the ytterbium atom to haptotropic rearrangements seems to play a crucial role in these transformations. The lack of data on the bonding strength of the ytterbium atom with indenyl, fluorenyl, and pentamethylcyclopentadienyl ligands and redox potentials of Yb(II) in complexes **1–3** does not allow us to evaluate the influence of these factors on the reaction pathway. Further work on this subject is being actively pursued at the moment.

Experimental Section. Preparation of $[\text{Yb}(\eta^5\text{-C}_9\text{H}_7)\{\text{N}(2,6\text{-}i\text{-Pr}_2\text{C}_6\text{H}_3)\text{CH}(\text{C}_9\text{H}_7)(\text{C}_5\text{H}_5\text{N})\}\{\text{N}(2,6\text{-}i\text{-Pr}_2\text{C}_6\text{H}_3)\text{NCH}(\text{C}_5\text{H}_5\text{N})\}]$ (5**).** A solution of **4** (0.53 g, 1.99 mmol) in THF (5 mL) was added to a solution of **1** (0.53 g, 0.96 mmol) in THF (20 mL), and the reaction mixture was heated to 60 °C for 0.5 h. THF was evaporated in vacuo, toluene (20 mL) was added, and the reaction mixture was stirred at 60 °C for 1 h. Volatile material was evaporated in vacuo, and another portion of toluene (20 mL) was added. After the mixture was stirred at 60 °C for an additional 2 h, the solvent was evaporated in vacuo and the deep green solid residue was recrystallized from a THF–hexane mixture at –20 °C. Decanting the mother liquor, washing the crystals with cold hexane, and drying in vacuo at room temperature for 20 min afforded deep green crystals of **5**: yield 0.55 g (61%). Anal. Calcd for $\text{C}_{54}\text{H}_{58}\text{N}_4\text{Yb}$ (936.08): C, 69.28;

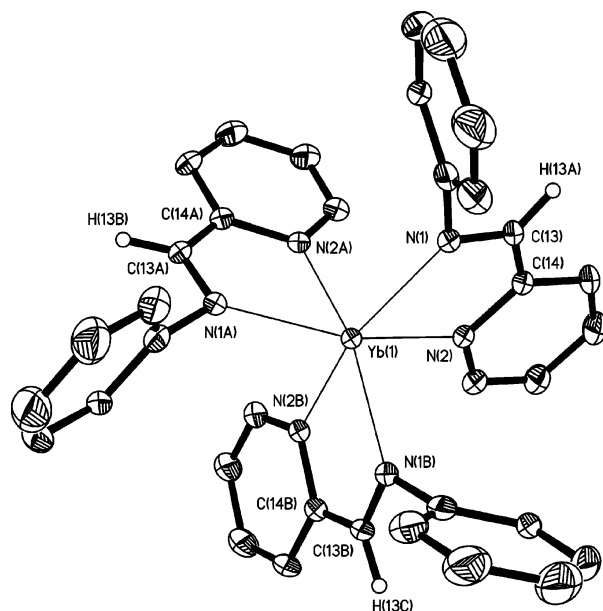
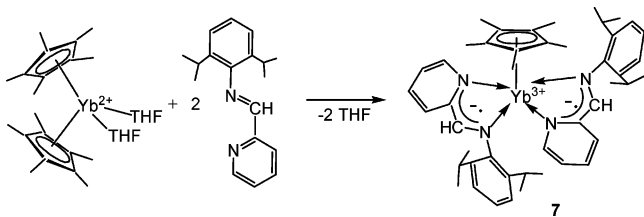


Figure 2. Molecular structure of the complex $[\text{Yb}\{(2,6\text{-}i\text{-Pr}_2\text{C}_6\text{H}_3)\text{NCH}(\text{C}_5\text{H}_5\text{N})\}_3]$ (**6**). Isopropyl groups of iminopyridine ligands are omitted for clarity. The terminal ellipsoids correspond to 30% probability. Selected bond lengths (Å): Yb1–N1 = 2.356(2), Yb1–N2 = 2.372(3), Yb1–C13 = 3.148(2), Yb1–C14 = 3.209(3), N1–C13 = 1.334(4), N2–C14 = 1.382(3), C13–C14 = 1.382(5).

H, 6.19; Yb, 18.48. Found: C, 68.89; H, 5.77; Yb, 18.80. IR (Nujol mull, cm^{-1}): 3060, 1620, 1600, 1565, 1275, 1169, 1103, 1046, 1015, 904, 768, 760, 750.

Preparation of $[\text{Yb}\{(2,6\text{-}i\text{-Pr}_2\text{C}_6\text{H}_3)\text{NCH}(\text{C}_5\text{H}_5\text{N})\}_3]$ (6**).** Similar to the procedure described for **5**, compound **6** was obtained from **4** (0.55 g, 2.06 mmol) in THF (5 mL) and **2** (0.67 g, 1.03 mmol) in THF (20 mL). The deep green solid residue was washed with hexane (2×15 mL). Fluorene (0.18 g, 80%) was found in the hexane extracts. Recrystallization from

Scheme 3



THF at $-20\text{ }^{\circ}\text{C}$ afforded deep green crystals of **6**: yield 0.35 g (52%). Anal. Calcd for $\text{C}_{54}\text{H}_{66}\text{N}_6\text{Yb}$ (972.17): C, 66.71; H, 6.78; Yb, 17.79. Found: C, 66.33; H, 6.54; Yb, 18.00. IR (Nujol mull, cm^{-1}): 3054, 1641, 1569, 1532, 1396, 1315, 1267, 1251, 1161, 1149, 992, 901, 801, 789, 738.

Preparation of $[\text{Yb}(\text{C}_5\text{Me}_5)\{(\text{2,6-}i\text{-Pr}_2\text{C}_6\text{H}_3\text{NCH}(\text{C}_5\text{H}_5\text{N})^-\}_2]$ (7**).** Similar to the procedure described for **5**, compound **7** was obtained from **4** (0.58 g, 2.18 mmol) in THF (5 mL) and **3** (0.64 g, 1.09 mmol) in THF (20 mL). Recrystallization of the greenish brown solid residue from hexane at $-20\text{ }^{\circ}\text{C}$ afforded greenish brown crystals of **7**: yield 0.67 g (74%). Anal. Calcd for $\text{C}_{46}\text{H}_{59}\text{N}_4\text{Yb}$ (841.01): C, 65.69; H, 7.01; Yb, 20.57. Found: C, 65.30; H, 6.73; Yb, 20.93. IR (Nujol mull, cm^{-1}): 3060, 1620, 1600, 1565, 1275, 1169, 1103, 1046, 1015, 904, 804, 768, 742, 662.

Crystal data for **5**: $\text{C}_{54}\text{H}_{58}\text{N}_4\text{Yb}$, $M_r = 936.08$, $T = 293(2)$ K, triclinic, $P\bar{1}$, $a = 11.2187(7)\text{ \AA}$, $b = 11.8654(8)\text{ \AA}$, $c = 18.0649(12)\text{ \AA}$, $\alpha = 90.087(2)^{\circ}$, $\beta = 90.889(2)^{\circ}$, $\gamma = 113.3530(10)^{\circ}$, $V = 2199.6(2)\text{ \AA}^3$, $Z = 2$, $\rho_{\text{calcd}} = 1.413\text{ Mg m}^{-3}$, $\mu = 2.167\text{ mm}^{-1}$, $F(000) = 960$, crystal size $0.04 \times 0.03 \times 0.02\text{ mm}$, $\theta = 1.88\text{--}25.00^{\circ}$, index ranges $-12 \leq h \leq 13$, $-14 \leq k \leq 14$, $-21 \leq l \leq 14$, 12 097 reflections collected, 7696 independent reflections, $R(\text{int}) = 0.0302$, $\text{GOF} = 0.952$, $R_1 = 0.0357$, $wR_2 = 0.0703$ ($I > 2\sigma(I)$), $R_1 = 0.0503$, $wR_2 = 0.0735$ (all data), largest difference peak/hole ($\rho_{\text{max}}/\rho_{\text{min}}$) $1.339/-0.554\text{ e \AA}^{-3}$.

Crystal data for **6**: $\text{C}_{54}\text{H}_{66}\text{N}_6\text{Yb}$, $M_r = 972.17$, $T = 100(2)$ K, rhombohedral, $R\bar{3}$, $a = 18.5730(8)\text{ \AA}$, $b = 18.5730(8)\text{ \AA}$, $c = 25.1943(15)\text{ \AA}$, $\alpha = \beta = 90.0^{\circ}$, $\gamma = 120.0^{\circ}$, $V = 7526.6(6)\text{ \AA}^3$, $Z = 6$, $\rho_{\text{calcd}} = 1.287\text{ Mg m}^{-3}$, $\mu = 1.904\text{ mm}^{-1}$, $F(000) = 3012$, crystal size $0.30 \times 0.30 \times 0.02\text{ mm}$, $\theta = 2.05\text{--}23.00^{\circ}$, index ranges $-19 \leq h \leq 20$, $-19 \leq k \leq 20$, $-27 \leq l \leq 27$, 11 474 reflections collected, 2310 independent reflections, $R(\text{int}) = 0.0353$, $\text{GOF} = 1.088$, $R_1 = 0.0304$, $wR_2 = 0.0824$ ($I > 2\sigma(I)$), $R_1 = 0.0365$, $wR_2 = 0.0850$ (all data), largest difference peak/hole ($\rho_{\text{max}}/\rho_{\text{min}}$) $0.915/-0.512\text{ e \AA}^{-3}$.

Crystal data for **7**: $\text{C}_{46}\text{H}_{59}\text{N}_4\text{Yb}$, $M_r = 841.01$, $T = 100(2)$ K, triclinic, $P\bar{1}$, $a = 10.8712(5)\text{ \AA}$, $b = 11.5312(5)\text{ \AA}$, $c = 17.6163(8)\text{ \AA}$, $\alpha = 74.0000(10)^{\circ}$, $\beta = 82.1300(10)^{\circ}$, $\gamma = 71.8730(10)^{\circ}$, $V = 2014.27(16)\text{ \AA}^3$, $Z = 2$, $\rho_{\text{calcd}} = 1.387\text{ Mg m}^{-3}$, $\mu = 2.358\text{ mm}^{-1}$, $F(000) = 866$, crystal size $0.27 \times 0.22 \times 0.09\text{ mm}$, $\theta = 1.92\text{--}29.21^{\circ}$, index ranges $-14 \leq h \leq 14$, $-15 \leq k \leq 15$, $-24 \leq l \leq 23$, 21 288 reflections collected, 10 535 independent reflections, $R(\text{int}) = 0.0242$, $\text{GOF} = 1.070$, $R_1 = 0.0299$, $wR_2 = 0.0701$ ($I > 2\sigma(I)$), $R_1 = 0.0356$, $wR_2 = 0.0723$ (all data), largest difference peak/hole ($\rho_{\text{max}}/\rho_{\text{min}}$) $2.710/-0.808\text{ e \AA}^{-3}$.

The data were collected on a SMART APEX diffractometer (graphite monochromated, Mo $\text{K}\alpha$ radiation, ω - φ scan technique, $\lambda = 0.71073\text{ \AA}$). The structures were solved by Patterson (**5**) and direct (**6**, **7**) methods and were refined on F^2 using the SHELXTL¹² package. All non-hydrogen atoms were refined anisotropically. In **5** hydrogen atoms were refined with mixed treatment. In complex **6** all hydrogen atoms were included into the model at geometrically calculated positions and refined using

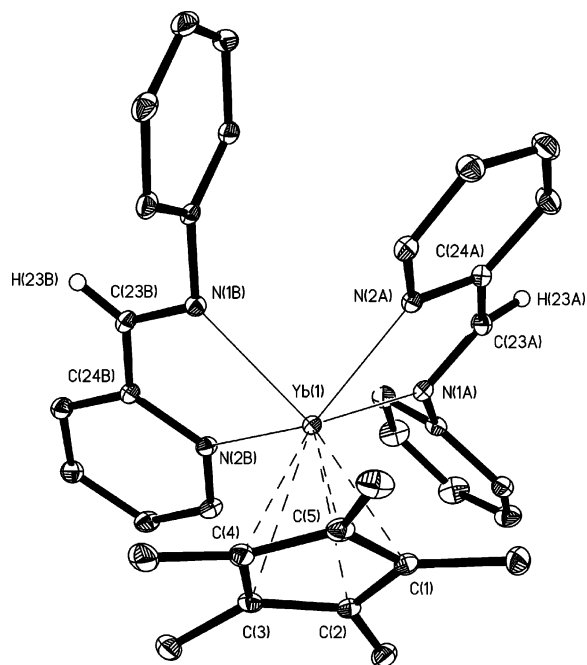


Figure 3. Molecular structure of the complex $[\text{Yb}(\text{C}_5\text{Me}_5)\{(\text{2,6-}i\text{-Pr}_2\text{C}_6\text{H}_3\text{NCH}(\text{C}_5\text{H}_5\text{N})^-\}_2]$ (**7**). Isopropyl groups of iminopyridine ligands are omitted for clarity. The terminal ellipsoids correspond to 30% probability. Selected bond lengths (\AA) and angles (deg): Yb1–C1 = 2.585(3), Yb1–C2 = 2.613(3), Yb1–C3 = 2.655(3), Yb1–C4 = 2.673(3), Yb1–C5 = 2.629(3), Yb–C_{av} = 2.631(3), Yb1–C23A = 3.142(3), Yb1–C23B = 3.130(3), Yb1–C24A = 3.180(2), Yb1–C24B = 3.173(3), Yb1–N1A = 2.356(2), Yb1–N2A = 2.345(2), Yb1–N1B = 2.346(2), Yb1–N2B = 2.333(2), N1A–C23A = 1.340(4), N2A–C24A = 1.380(3), C23A–C24A = 1.407(4), N1B–C23B = 1.342(3), N2B–C24B = 1.381(3), C23B–C24B = 1.409(4); N2B–Yb1–N1B = 71.80(7), N2A–Yb1–N1A = 71.92(8).

a riding model. The isotropic displacement parameters of all hydrogen atoms were fixed to 1.2 times the U value of the atoms they are linked to (1.5 times for methyl groups). The H atoms in **7** were located from Fourier synthesis and refined isotropically. SADABS¹³ was used to perform area-detector scaling and absorption corrections. The CCDC files 627244 (**5**), 627245 (**6**), and 627246 (**7**) contain supplementary crystallographic data for this paper. These data can be obtained free of charge at www.ccdc.cam.ac.uk/const/retrieving.html from the Cambridge Crystallographic Data Centre, 12 Union Road, Cambridge CB2 1EZ, U.K. (fax, (internat.) +44-1223/336-033; e-mail, deposit@ccdc.cam.ac.uk).

Acknowledgment. This work was supported by the Russian Foundation for Basic Research (Grant Nos. 05-03-32390, 06-03-32728-a, 06-03-81005 Bel). Contract No. 02.445.11.7365 of the Federal Science and Innovation Agency, the Program of the Presidium of the Russian Academy of Science (RAS), and the RAS Chemistry and Material Science Division, the Grant of President of Russian Federation supporting scientific schools (No. 8017.2006.3). A.T. thanks the Russian Foundation for science support.

Supporting Information Available: CIF files giving crystallographic data, including bond lengths and angles, of compounds **5**–**7**. This material is available free of charge via the Internet at <http://pubs.acs.org>.

OM070073S

(12) SMART: Bruker Molecular Analysis Research Tool, v. 5.625; Bruker AXS, Madison, WI, 2000.

(13) Sheldrick, G. M. SADABS: Bruker/Siemens Area Detector Absorption Correction Program, v.2.01; Bruker AXS, Madison, WI, 1998.